Novel Recombinant Hemoglobin, rHb (βN108Q), with Low Oxygen Affinity, High Cooperativity, and Stability against Autoxidation†

Ching-Hsuan Tsai, Tsuei-Yun Fang,‡ Nancy T. Ho, and Chien Ho*

Department of Biological Sciences, Carnegie Mellon University, 4400 Fifth Avenue, Pittsburgh, Pennsylvania 15213

Received May 16, 2000; Revised Manuscript Received August 3, 2000

ABSTRACT: Using our *Escherichia coli* expression system, we have constructed rHb (βN108Q), a new recombinant hemoglobin (rHb), with the amino acid substitution located in the $\alpha_1\beta_1$ subunit interface and in the central cavity of the Hb molecule. rHb (βN108Q) exhibits low oxygen affinity, high cooperativity, enhanced Bohr effect, and slower rate of autoxidation of the heme iron atoms from the Fe^{2+} to the Fe^{3+} state than other low-oxygen-affinity rHbs developed in our laboratory, e.g., rHb (αV96W) and rHb (αV96W, βN108K). It has been reported by Olson and co-workers [Carver et al. (1992) *J. Biol. Chem. 267*, 14443−14450; Brantley et al. (1993) *J. Biol. Chem. 268*, 6995−7010] that the substitution of phenylalanine for leucine at position 29 of myoglobin can inhibit autoxidation in myoglobin and at position 29 of the α-chain of hemoglobin can lower NO reaction in both the deoxy and the oxy forms of human normal adult hemoglobin. Hence, we have further introduced this mutation, αL29F, into βN108Q. rHb (αL29F, βN108Q) is stabilized against auto- and NO-induced oxidation as compared to rHb (βN108Q), but exhibits lower oxygen affinity at pH below 7.4 and good cooperativity as compared to Hb A. Proton nuclear magnetic resonance (NMR) studies show that rHb (βN108Q) has similar tertiary structure around the heme pockets and quaternary structure in the $\alpha_1\beta_1$ and $\alpha_1\beta_2$ subunit interfaces as compared to those of Hb A. The tertiary structure of rHb (αL29F, βN108Q) as measured by ^{1}H NMR, especially the α-chain heme pocket region (both proximal and distal histidyl residues), is different from that of CO- and deoxy-Hb A, due to the amino acid substitution at αL29F. ^{1}H NMR studies also demonstrate that rHb (βN108Q) can switch from the R quaternary structure to the T quaternary structure without changing ligation state upon adding an allosteric effector, inositol hexaphosphate, and reducing the temperature. On the basis of its low oxygen affinity, high cooperativity, and stability against autoxidation, rHb (βN108Q) is considered a potential candidate for the Hb-based oxygen carrier in a blood substitute system.

In our laboratory, we have developed an expression system to produce authentic human normal adult hemoglobin (Hb A)[1] in good yield in *Escherichia coli* (*1*, *2*). With this expression system, we have designed and expressed mutant Hbs with low oxygen affinity and high cooperativity (*3*−*5*), which are the desired properties of recombinant (r) Hbs that may be used as potential Hb-based oxygen carriers and Hb therapeutics in a blood substitute system. A unique feature of this class of rHbs is that their R (ligated) quaternary structure can be switched to the T (unligated) structure, without changing the ligation state of the Hb molecule, by lowering the ambient temperature and/or by adding an allosteric effector, such as inositol hexaphosphate (IHP). rHb (αV96W) (*3*) is the first low-oxygen-affinity mutant rHb with high cooperativity developed in our laboratory. rHb (αV96W, βN108K) was constructed based on αV96W and a naturally occurring low-oxygen-affinity mutant, Hb Presbyterian (βN108K). rHb (αV96W, βN108K) is of particular interest because it has good cooperativity and the lowest oxygen affinity of rHbs studied in our laboratory (*5*). rHb (αV96W, βN108K) has also been shown to have the greatest tendency to switch from the R quaternary structure to the T quaternary structure without changing its ligation state (*5*).

However, the ease of autoxidation of rHb (αV96W, βN108K) makes it less desirable as an Hb-based oxygen carrier in a blood substitute system. Natural mutant Hbs with low oxygen affinity are known to exhibit an increased rate of autoxidation (*6*, *7*). The oxidation rate appears to be inversely proportional to the oxygen affinity of Hbs (*8*). This correlation between the oxygen affinity and the autoxidation rate poses a serious challenge for engineering Hb-based oxygen carriers since stability against autoxidation is compromised by the need for lower oxygen affinity. When Hb is in the extracellular environment of blood vessels, due to the lack of allosteric effectors, such as 2,3-bisphosphoglycerate (2,3-BPG), low oxygen affinity with high cooperativity is required for efficient oxygen delivery. It has been reported by Olson and co-workers (*9*−*13*) that the mutation L29F at the B10 position can inhibit autoxidation in myoglobin and

† This work was supported by research grants from the National Institutes of Health (R01HL-24525, R01HL-58249, and S10RR-11248). C.-H.T. was supported by an Affiliate Student Award (T9902P) from the Pennsylvania Affiliate of the American Heart Association.

* Address all correspondence to this author. Telephone: 412-268-3395. Fax: 412-268-7083. E-mail: chienho@andrew.cmu.edu.

‡ Present address: Institute of Molecular Biology, Academia Sinica, Taipei, Taiwan.

[1] Abbreviations: Hb A, human normal adult hemoglobin; rHb, recombinant hemoglobin; met-Hb, methemoglobin; Mb, myoglobin; NMR, nuclear magnetic resonance; DSS, 2,2-dimethyl-2-silapentane-5-sulfonate; IHP, inositol hexaphosphate; 2,3-BPG, 2,3-bisphosphoglycerate; EDTA, ethylenediaminetetraacetate; k', CO-binding constant; k_{off}, CO dissociation constant; $k'_{oxy,NO}$, NO-induced oxidation rate constant; k_{auto}, autoxidation rate constant.

10.1021/bi001116a CCC: $19.00
Published on Web 10/14/2000

that at the B10 position of the α-chain can lower NO reaction with deoxy- and oxy-Hb A. In an effort to construct a blood substitute prototype, Jeong et al. (*14*) introduced the mutation αL29F into rHb (αV96W, *β*N108K) and constructed a triple mutant, rHb (αL29F, αV96W, *β*N108K). This rHb is more stable against autoxidation than rHb (αV96W, *β*N108K) but still exhibits low oxygen affinity and good cooperativity, suggesting that αL29F is effective in stabilizing Hb against autoxidation. However, the oxidized form of rHb (αL29F, αV96W, *β*N108K) exhibits hemichrome-like spectra (*14*). Hemichrome forms when methemoglobin (met-Hb) converts from the high-spin ferric form to the low-spin ferric form in which the distal imidazole displaces the H_2O ligand (*15*−*17*).

*β*108 (G10) is located in the $\alpha_1\beta_1$ subunit interface and in the central cavity of the Hb molecule (*6*). The side chain of Asn in the G10 position interacts freely with the water molecules of the central cavity in both the deoxy and the oxy forms (*18*, *19*). There are four known Hb variants with a single amino acid substitution at *β*108: Hb Presbyterian (*β*N108K) (*20*), Hb Yoshizuka (*β*N108D) (*21*), Hb Shizuka (*β*N108H) (*22*), and Hb Schlierbach (*β*N108I) (*23*). Hb Presbyterian (*β*N108K) and Hb Yoshizuka (*β*N108D) both exhibit low oxygen affinity and high cooperativity (*5*, *20*, *24*), despite the fact that the amino acid substitutions of these two mutants have an opposite charge. Previous studies on the oxygen-binding properties of rHb Presbyterian (*β*N108K) and rHb Yoshizuka (*β*N108D) suggest that mechanisms other than the buildup of excess positive charges in the central cavity of the Hb molecule contribute to the oxygenation properties of rHb Presbyterian (*5*). We have also shown that electrostatic interactions in the central cavity of Hb play an important role in regulating the oxygen-binding properties of Hb molecules (*5*). There are no functional studies published on Hb Shizuka (*β*N108H) (*22*) yet, while Hb Schlierbach (*β*N108I) is reported to be a low-oxygen-affinity variant (*23*). It is noted that an amino acid substitution at *β*108 with either charged or hydrophobic residues (Lys and Asp versus Ile) results in low-oxygen-affinity variants. In an attempt to control the oxygen affinity of rHbs with cooperativity preserved and to clarify the functional role of *β*108Asn as well, we have constructed rHb (*β*N108Q), rHb (*β*N108R), rHb (*β*N108E), and rHb (*β*N108A), which exhibit 1.7−2.3-fold lower oxygen affinity than that of Hb A with cooperativity preserved (C.-H. Tsai, N. T. Ho, and C. Ho, unpublished results). Amino acid substitutions with either charged polar (Asp, Glu, Arg, Lys) or uncharged polar (Gln) or even hydrophobic (Ala) side chains at *β*108Asn result in lower oxygen affinity and good cooperativity. This suggests the topographical significance of *β*108Asn in regulating the oxygen-binding properties of Hb A.

All rHbs having amino acid substitutions at the *β*108 site that we have studied so far exhibit low oxygen affinity and high cooperativity. On the basis of the oxygen-binding measurements of rHbs mutated at the *β*108 site, rHb (*β*N108Q) is the most stable against autoxidation, i.e., there is no met-Hb formation upon oxygenation during the oxygen-binding measurements. In an effort to construct a blood substitute prototype, we have further introduced the mutation αL29F into *β*N108Q. It was hoped that rHb (αL29F, *β*N108Q) would exhibit low oxygen affinity and high cooperativity, but also possess added properties, i.e., be more stable against NO-induced oxidation and autoxidation. Here, we report the oxygen-binding equilibrium, CO-binding rate constant, CO-dissociation rate constant, and NO-induced oxidation properties of these two rHbs, rHb (*β*N108Q) and rHb (αL29F, *β*N108Q). We have also compared the autoxidation properties of rHb (*β*N108Q) and rHb (αL29F, *β*N108Q) with other known low-oxygen-affinity rHbs, such as rHb (αV96W), rHb (αV96W, *β*N108K), and rHb (αL29F, αV96W, *β*N108K). The unique functional properties of rHb (*β*N108Q) are the low oxygen affinity, high cooperativity, and stability against autoxidation as compared to other low-oxygen-affinity rHbs developed in this laboratory. ^{1}H NMR studies were conducted to investigate the tertiary and quaternary structures of rHb (*β*N108Q) and rHb (αL29F, *β*N108Q). These studies show that the R quaternary structure of rHb (*β*N108Q) can be switched to the T quaternary structure without changing its ligation state when the temperature is lowered and the allosteric effector, IHP, is added, suggesting that rHb (*β*N108Q) has a more stable T structure than that of Hb A. Thus, these properties make rHb (*β*N108Q) a very attractive candidate as a potential Hb-based oxygen carrier in a blood substitute system.

MATERIALS AND METHODS

Construction of Expression Plasmids. The *Escherichia coli* Hb expression plasmid, pHE2, was constructed in our laboratory (*1*) and forms the basis for constructing other plasmids for expressing mutant Hbs. The synthetic human *β*-globin gene from plasmid pHE2 was inserted into plasmid pALTER-1 by the method of the Altered Sites II in-vitro Mutagenesis System (Promega). Synthetic oligonucleotide 5′-CGTCTGCTGGGT*CAG*GTACTAGTTTGCG-3′ was used as a primer to introduce the mutation *β*N108Q. This oligonucleotide was obtained from DNA International Inc. (Lake Oswego, Oregon). The human normal *β*-globin gene in plasmid pHE2 was then replaced by the mutated *β*-globin gene to produce pHE2009. The plasmid (pHE284) for the expression of rHb (αL29F) was reported previously (*14*). The plasmid pHE2018 for the expression of rHb (αL29F, *β*N108Q) was constructed by ligation of the 6.06-kb *Pst*I−*Bam*HI fragment of pHE2009 and the 0.79-kb *Bam*HI−*Pst*I fragment of pHE284.

Chemicals and restriction enzymes were purchased from major suppliers, such as Fisher, Sigma, Bio-Rad, Boehringer Mannheim, New England BioLabs, Pharmacia, Promega, and United States Biochemicals and were used without further purification.

Growth of Cells. E. coli cells were grown in a 10-L Microferm fermentor (New Brunswick Scientific, model BioFlo 3000) at 32 °C until the optical density at 600 nm reached 10. Expression of rHbs was induced by adding isopropyl *β*-thiogalactopyranoside (Sigma) to 0.1−0.4 mM. The culture was then supplemented with hemin (20−50 mg/L), and the growth was continued for at least 4 h. The cells were harvested by centrifugation and stored frozen at −80 °C until needed for purification. For details, refer to Shen et al. (*1*, *2*).

Isolation and Purification of rHbs. The purification of rHbs followed the procedures described previously (*1*, *2*). In the first step after the cell lysis procedure, the supernatant

from the lysate was left at 30 °C overnight (*5*). Following the procedures developed in our laboratory (*1*, *2*), the rHb fraction collected after the Q-Sepharose Fast-Flow column (Pharmacia anion exchanger) was oxidized, reduced, and converted to the CO form. This Hb solution was then purified by eluting from a fast protein liquid chromatography Mono-S column (Pharmacia Cation Exchanger, HR 16/10).

The electrospray ionization mass spectrometric analyses were performed on a VG Quattro-BQ (Fisons Instruments, VG Biotech, Altrincham, U.K.) as previously described (*1*). Automated cycles of Edman degradation were performed on an Applied Biosystems gas/liquid-phase sequencer (model 470/900A) equipped with an on-line phenylthiohydantoin amino acid analyzer (model 120A) as previously described (*1*). These two analytical procedures were used to assess the quality of our rHbs. All rHbs used in this study had the correct molecular weights and contained less than 1% of methionine at the amino termini.

Oxygen-Binding Properties of rHbs. The oxygen dissociation curves of rHbs were measured on a Hemox-Analyzer (TCS Medical Products, Huntington Valley, PA) at 29 °C as a function of pH in 0.1 M sodium phosphate buffer. The concentration of Hb used in this study was about 0.1 mM (in terms of heme). The met-Hb reductase system was used (*25*). A visible absorption spectrum of each sample was recorded immediately after the oxygen equilibrium measurement, and the met-Hb content was estimated by using the extinction coefficients for Hb reported by Antonini (*26*). Oxygen equilibrium parameters were derived by fitting the Adair equations to each equilibrium oxygen-binding curve by a nonlinear least-squares procedure. P_{50}, a measure of oxygen affinity, was obtained at 50% saturation. The Hill coefficient (n_{max}), a measure of cooperativity, was determined from the maximum slope of the Hill plot by linear regression. n_{max} was derived between 60% and 65% oxygen saturation. The accuracy of P_{50} measurements (in mmHg) is ±5% and that of n_{max} is ±7%.

Kinetic Measurements. All of the rapid mixing experiments were performed using an OLIS stopped-flow apparatus (OLIS, Bogart, GA) (with a dead time of ≈3 ms). The temperature was controlled at 20 °C with a circulating water bath and monitored with a thermometer. To maintain anaerobic conditions in the stopped-flow apparatus, a 10-mL solution of degassed 0.1 M sodium phosphate buffer at pH 8.5 containing 10 mg of dithionite was loaded into the stopped-flow system the day before the kinetic measurements. The water bath in the stopped-flow apparatus was bubbled with Ar gas overnight and during the experiments. Before the samples were loaded, a 20-mL solution of degassed 0.1 M sodium phosphate buffer at pH 7.0 was used to wash the stopped-flow system.

CO-Binding Reaction. For the CO-binding reactions, deoxy-Hb samples (20 μM heme before mixing) were reacted with CO-saturated 0.1 M phosphate buffer at pH 7.0 (1 mM before mixing), and the reaction was monitored at 440 nm. The reactions were carried out in the presence and absence of 50 μM IHP. The time courses were fitted with one exponential decay to determine the observed rate (k_{obs}). Under the reaction conditions, the reaction is pseudo-first-order, and the bimolecular association rate constants were obtained by dividing the observed rate constants by the CO concentration ($k' = k_{obs}/[CO]$).

CO Displacement by NO Reactions. The off-rate of HbCO samples was determined by mixing HbCO with saturated NO solution[2] (*27*, *28*). A saturated solution of NO was mixed anaerobically with an equal volume of a 20 μM (heme) protein solution. The final concentration of NO was 1 mM and of protein was 10 μM. The reaction was monitored at 440 nm, and the observed rates were determined by fitting the traces to a single-exponential decay.

NO-Induced Oxidation Reactions. Solutions of oxygen-equilibrated Hb were mixed with anaerobic solutions of NO, and the met-Hb formation was monitored as absorbance increases at 402 nm. The value of the bimolecular rate constant for this reaction is reported to be extremely large, on the order of 10 μM^{-1} s^{-1} (*11*), so the concentration of NO after mixing was kept low (≤10 μM) to prevent the reaction from going to completion during the dead time of the instrument (3 ms). As a result, very low protein concentrations (0.4 μM heme after mixing) were required to maintain a pseudo-first-order approximation. The low Hb concentrations resulted in small absorbance changes, and an averaging of 10−14 traces was necessary to enhance the signal-to-noise ratio. The time courses were fitted to a single-exponential expression using an iterative nonlinear least-squares algorithm to obtain the observed rate constants. The bimolecular rate constants were obtained by dividing the observed rate constants by the NO concentration ($k'_{oxy,NO} = k_{obs}/[NO]$).

^{1}H NMR Investigation of rHbs. ^{1}H NMR spectra of rHbs were obtained from Bruker AVANCE DRX-300 and AVANCE DRX-500 NMR spectrometers. All Hb samples were in 0.1 M sodium phosphate buffer in 100% water, and the Hb concentration was about 5% (∼0.8 mM in terms of heme). The water signal was suppressed by using a jump-and-return pulse sequence (*29*). Proton chemical shifts are referenced to the methyl proton resonance of 2,2-dimethyl-2-silapentane-5-sulfonate (DSS) indirectly by using the water signal, which occurs at 4.76 ppm downfield from that of DSS at 29 °C, as the internal reference.

Autoxidation of rHbs. The autoxidation was recorded by monitoring the rate of disappearance of the oxy-marker (−2.34 ppm from DSS) (*30*, *31*) on the Bruker AVANCE DRX-300. The autoxidation reaction was carried out in PlasmaLyte buffer (Baxter) in the presence of 5% D_2O and 5 mM ethylenediaminetetraacetate (EDTA) at pH 7.4 and at 37 °C. The HbO_2 concentration was 5% (∼0.8 mM).

RESULTS

Functional Studies

Oxygen-Binding Properties of rHbs. Figure 1 shows the oxygen-binding measurements of rHb (αL29F), rHb (βN108Q), rHb (αL29F, βN108Q), and Hb A in 0.1 M sodium phosphate buffer as a function of pH at 29 °C. rHb (βN108Q) exhibits a significantly lower oxygen affinity as

[2] Stock solutions of NO were prepared by injecting anaerobic buffer solution (0.1 M phosphate at pH 7.0) into a gas-tight tonometer, which had been flushed with 1 atm of NO. The NO gas used had been passed through a column of KOH pellets to remove acids (NO_2). Anaerobic buffer solution was prepared by bubbling the solution with argon gas for at least 30 min. Solutions at lower NO concentration were prepared by dilution of the saturated NO solution with an appropriate volume of an anaerobic buffer solution.

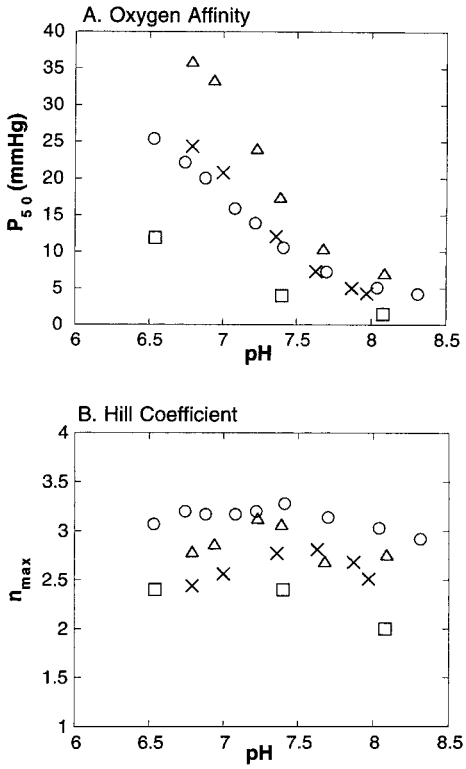

FIGURE 1: pH dependence of the oxygen affinity (P_{50}) (A) and the Hill coefficient (n_{max}) (B) in 0.1 M phosphate buffer at 29 °C: (○) Hb A; (□) rHb (αL29F); (△) rHb (βN108Q); (×) rHb (αL29F, βN108Q). Oxygen dissociation data were obtained with 0.1 mM Hb and in the presence of a reductase system (*25*).

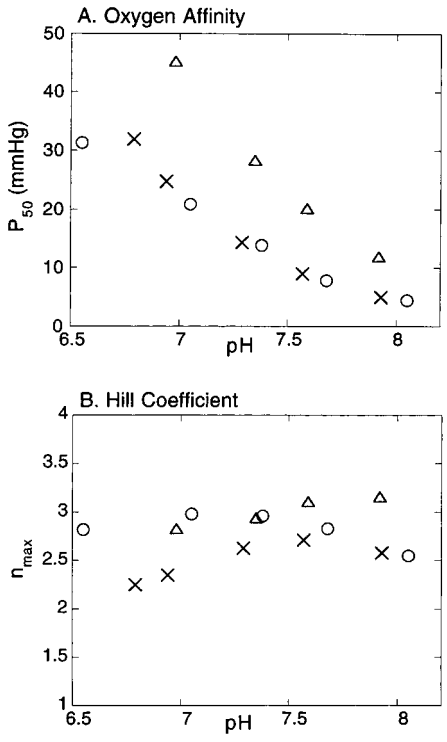

FIGURE 2: pH dependence of the oxygen affinity (P_{50}) (A) and the Hill coefficient (n_{max}) (B) in 0.1 M phosphate buffer in the presence of 5 mM 2,3-BPG at 29 °C: (○) Hb A; (△) rHb (βN108Q); (×) rHb (αL29F, βN108Q). Oxygen dissociation data were obtained with 0.1 mM Hb and in the presence of a reductase system (*25*).

compared to that of Hb A over the pH range from 6.79 to 8.09. The oxygenation process of rHb (βN108Q) is very cooperative, with an n_{max} value of about 2.7−3.1 depending on the pH as compared to about 3.2 for Hb A. On the other hand, the mutation at the α-chain B10 position, i.e., αL29F, increases the oxygen affinity and decreases the cooperativity. rHb (αL29F, βN108Q) shows slightly higher P_{50} values as compared to those of Hb A at pH <7.4, suggesting that the effect of the mutations on the oxygen affinity is additive. rHb (αL29F, βN108Q) preserves cooperativity in binding of oxygen with an n_{max} value of 2.4−2.8. Figure 2 shows the decrease in oxygen affinity induced by the presence of 2,3-BPG. Over the pH range we measured in the presence of 2,3-BPG, rHb (βN108Q) exhibits low oxygen affinity and high cooperativity, while rHb (αL29F, βN108Q) exhibits similar oxygen affinity to Hb A. In addition to low oxygen affinity and high cooperativity, the oxygen-binding curve of rHb (βN108Q) shows a unique property, as seen in Figure 3. At low oxygen pressure, the saturation percentage of oxy-rHb (βN108Q) is much lower than that of oxy-Hb A, suggesting that the first oxygen binds with much lower affinity to rHb (βN108Q). Figure 3 also shows that the oxygen affinity of rHb (βN108Q) measured in the absence of 2,3-BPG is lower than that of Hb A in the presence of 5 mM 2,3-BPG, making it a potential candidate for an oxygen carrier in a blood substitute system. Figures 1 and 2 show that the alkaline Bohr effect (which in Hb A results in a decrease in oxygen affinity with a lowering of the pH) is enhanced in rHb (βN108Q) and rHb (αL29F, βN108Q) as compared to Hb A. Table 1 compares the number of Bohr protons released upon oxygenation per heme calculated from the linkage equation (*32*, *33*): $\Delta H^+ = -\partial \log P_{50}/\partial \mathrm{pH}$. Both rHb ($\beta$N108Q) and rHb (αL29F, βN108Q) release more Bohr protons than Hb A in the presence and absence of the allosteric effector, 2,3-BPG.

CO-Binding Constants. Figure 4 shows the normalized time courses for the CO-binding reaction with deoxy-rHbs and deoxy-Hb A. The association rate constants are presented in Table 2. The mutation in rHb (βN108Q) causes a 1.2-fold decrease in the initial rate of CO binding. Substitution of a bulky side chain (Phe) for Leu at the B10 position on the α-chain lowers the initial CO-binding constant by 4.5-fold. rHb (αL29F, βN108Q) shows a 5.7-fold decrease in the initial CO-binding constant, possibly because the effect of mutations to Gln at β108 and to Phe at α29 is additive. The IHP effect on the initial rate constants of CO binding to rHbs is also shown in Table 2. Hb A shows a decrease in the initial CO-binding rate constant by 1.7-fold in the presence of IHP, suggesting that IHP is capable of stabilizing the T state of Hb A. The effect of IHP in slowing down the initial CO binding is about the same in rHb (βN108Q), but increased slightly in rHb (αL29F) and rHb (αL29F, βN108Q). These results suggest that the mutation at αL29F enhances the IHP effect by destabilizing the deoxy structure.

CO-Dissociation Constants. The CO-dissociation rates for rHbs and Hb A were determined by a ligand displacement reaction with NO (*27*, *28*). The dissociation rate constants (off-rate) determined for rHbs and Hb A are listed in Table 2. The mutation in βN108Q results in a 1.2-fold increase in the CO-dissociation constant as compared to Hb A. rHb (αL29F) and rHb (αL29F, βN108Q), although they have 4.5−5.7-fold decreases in initial CO-binding rate constants as seen in Table 2, exhibit essentially the same CO-dissociation rate constants as Hb A.

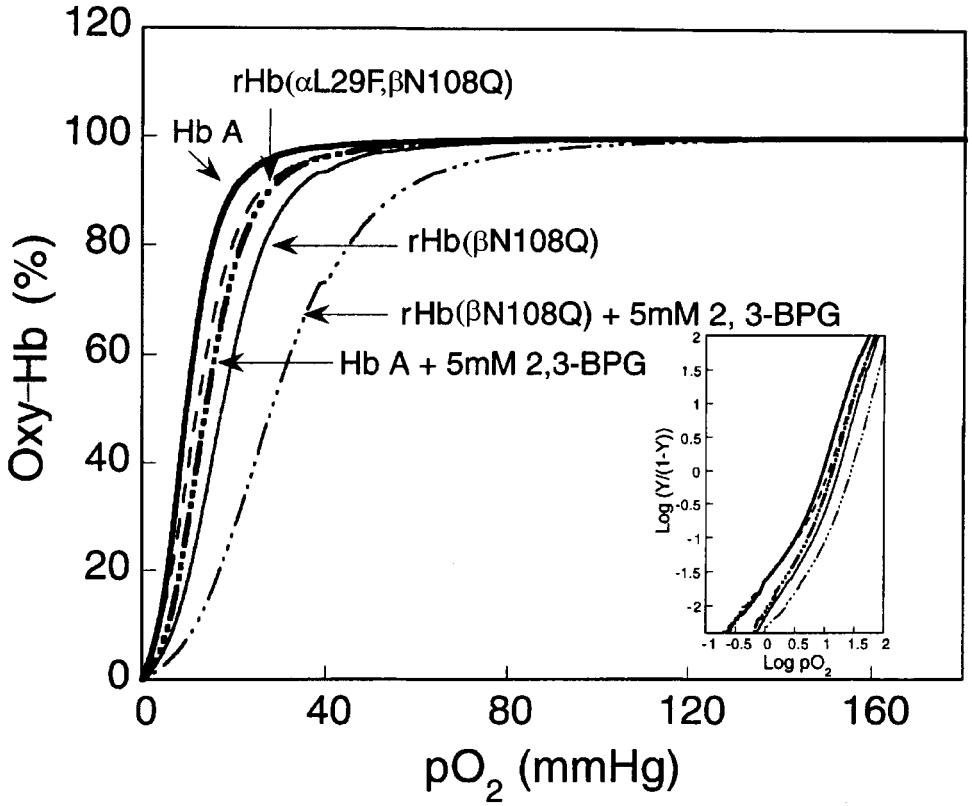

FIGURE 3: Oxygen-binding curves of Hb A, rHb (βN108Q), and rHb (αL29F, βN108Q) in 0.1 M phosphate buffer at pH 7.4 and 29 °C with and without 5 mM 2,3-BPG. The insert shows the Hill plots. Hb concentration was 0.1 mM heme. Oxygen dissociation data were obtained in the presence of a reductase system (*25*).

Table 1: Bohr Effect of Hb A, rHb (βN108Q), and rHb (αL29F, βN108Q) in 0.1 M Sodium Phosphate Buffer in the Absence and Presence of 5 mM 2,3-BPG at 29 °C[a]

hemoglobin	$\partial \log P_{50}/\partial$ pH in 0.1 M phosphate	$\partial \log P_{50}/\partial$ pH in 0.1 M phosphate + 5 mM BPG
Hb A	0.48 (pH 6.59−8.00)	0.58 (pH 6.55−8.05)
rHb (βN108Q)	0.56 (pH 6.79−8.09)	0.62 (pH 6.98−7.92)
rHb (αL29F, βN108Q)	0.67 (pH 6.79−7.97)	0.71 (pH 6.79−7.93)

[a] All the data are taken in the presence of a reductase system (*25*). The values of the Bohr effects reported here are the best estimates of the maximum Bohr effect in the pH range indicated in parentheses.

NO-Induced Oxidation. We have also measured the NO-induced oxidation rates of Hb A and rHbs. Figure 5 shows the normalized time courses for Hb A, rHb (βN108Q), and rHb (αL29F, βN108Q). The bimolecular rate constants are presented in Table 2. rHb (βN108Q) has an NO-induced oxidation rate increased by 1.3-fold as compared to that of Hb A. rHb (αL29F) and rHb (αL29F, βN108Q) have 12- and 15-fold decreases in the rate constant for NO-induced oxidation as compared to that of Hb A, respectively. Eich et al. (*11*) reported rate constants in the range of 30−50 and 3 μM^{-1} s^{-1} for Hb A and rHb (αL29F), respectively. Rohlfs et al. (*35*) reported that Hb A has a $k'_{ox,NO}$ value of 30 μM^{-1} s^{-1}. Though these $k'_{ox,NO}$ values are slightly larger than the values obtained in this study, it is apparent that the effect of αL29F in slowing down the NO-induced oxidation of Hb A reported here agrees with that suggested by Eich et al. (*11*).

Autoxidation. We have monitored the autoxidation process of oxy-Hb A, oxy-rHb (βN108Q), oxy-rHb (αL29F, βN108Q), and three other known low-oxygen-affinity mutants, oxy-rHb (αV96W), oxy-rHb (αV96W, βN108K), and oxy-rHb (αL29F, αV96W, βN108K), by ^{1}H NMR. The resonance at −2.34 ppm upfield from DSS has been assigned to the γ_2-CH_3 of E11Val of Hb A in the oxy form (*30*, *31*). Monitoring the rate of disappearance of this oxy-marker as a function of time allows us to determine the autoxidation rate of our Hb samples (Figure 6). The percentage of ferrous Hb varies with time (t) monoexponentially, and the autoxidation rate constant can be obtained from $[\text{ferrous-Hb}]_t = [\text{ferrous-Hb}]_{t=0} \times \exp(-k_{auto}t)$, where k_{auto} is the autoxidation rate constant. The autoxidation rate constants of Hb A and rHbs are listed in Table 3. At pH 7.4 and 37 °C in PlasmaLyte buffer, rHb (αV96W, βN108K), rHb (αV96W), rHb (αL29F, αV96W, βN108K), rHb (βN108Q), and rHb (αL29F, βN108Q) autoxidized 7.9, 4.4, 2.8, 2.8, and 1.1 times faster than Hb A. The autoxidation rate is slowed by introducing the mutation αL29F. rHb (αL29F, βN108Q) and rHb (αL29F, αV96W, βN108K) autoxidized 2.5 and 2.7 times slower than rHb (βN108Q) and rHb (αV96W, βN108K), respectively. Thus, the mutation αL29F is very effective in slowing down the autoxidation process as suggested by the results on Mb (*9*).

Structural Studies

^{1}H NMR is an excellent tool for monitoring changes in the tertiary and quaternary structures of Hb A and its variants (*1*−*5*, *36*−*40*). Figure 7 shows the exchangeable proton resonances and the ring-current-shifted resonances of Hb A, rHb (βN108Q), and rHb (αL29F, βN108Q) in the CO form measured at 500 MHz. The ring-current-shifted resonances are sensitive to the orientation and/or conformation of the heme group relative to the amino acid residues in the heme pockets, i.e., the tertiary structure of the Hb molecule (*36*).

Table 2: Summary of CO-Binding Constants (k'), CO-Dissociation Constants (k_{off}), and NO-Induced Oxidation Rate Constants ($k'_{ox,NO}$)

hemoglobin	k' (μM^{-1} s^{-1})[a] − IHP	k' (μM^{-1} s^{-1})[a] + IHP	k_{off}[b] (s^{-1})	$k'_{ox,NO}$[c] (μM^{-1} s^{-1})
Hb A	0.170 ± 0.003[d,e]	0.103 ± 0.002[d,e]	0.0059 ± 0.0002[f]	21[g,h]
rHb (βN108Q)	0.136 ± 0.003	0.088 ± 0.003	0.0073 ± 0.0002	26
rHb (αL29F)	0.038 ± 0.002[d]	0.021 ± 0.002[d]	0.0060 ± 0.0003	1.7[g]
rHb (αL29F, βN108Q)	0.030 ± 0.001	0.014 ± 0.001	0.0064 ± 0.0005	1.4

[a] Reaction of deoxy-Hb with CO in 0.1 M sodium phosphate buffer at pH 7.0 and 20 °C. Rate constants obtained at [Hb] = 10 μM heme and [CO] = 500 μM after mixing in the absence and presence of 50 μM IHP (after mixing). [b] Reaction of CO-Hb with NO in 0.1 M sodium phosphate buffer at pH 7.0 and 20 °C. Rate constants obtained at [Hb] = 10 μM heme and [NO] = 1 mM after mixing. [c] Reaction of oxy-Hb with NO in 0.1 M sodium phosphate buffer at pH 7.0 and 20 °C. Rate constants obtained at [Hb] = 0.4 μM heme and [NO] = 1, 2, 4, and 5 μM after mixing.[d] k' for Hb A and rHb (αL29F) in 0.1 M phosphate buffer at pH 7.0 and 20 °C is 0.194 and 0.098 μM^{-1} s^{-1} (*14*). k' for Hb A and rHb (αL29F) under the same experimental conditions and in the presence of 2 mM IHP is 0.116 and 0.049 μM^{-1} s^{-1} (*14*). [e] k' for Hb A in the absence and presence of 25 μM IHP in 0.1 M KCl and 0.1 M Bis−Tris, pH 7.0, and 20 °C is 0.19 and 0.10 μM^{-1} s^{-1} (*34*). [f] k_{off} for Hb A is 0.0055 s^{-1} in 0.1 M KCl and 0.1 M Bis−Tris, pH 7.0, and 20 °C (*27*). [g] $k'_{oxy,NO}$ for Hb A and rHb (αL29F) is 50 and 3 μM^{-1} s^{-1} (*11*) as determined in 0.1 M sodium phosphate at pH 7.4 and 20 °C. [h] $k'_{oxy,NO}$ for Hb A is 30 μM^{-1} s^{-1} (*35*) as determined in 0.1 M Bis−Tris and 0.1 M Cl^-, pH 7.4, and 23 °C.

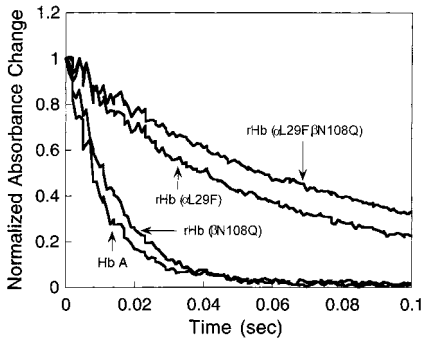

FIGURE 4: Normalized time courses for the reaction of deoxy-Hb with saturated CO in 0.1 M sodium phosphate buffer at pH 7.0 and 20 °C. All reactions were monitored at 440 nm in the stopped-flow apparatus as described in Materials and Methods. Hb concentration was 10 μM after mixing, and CO concentration was 0.5 mM after mixing.

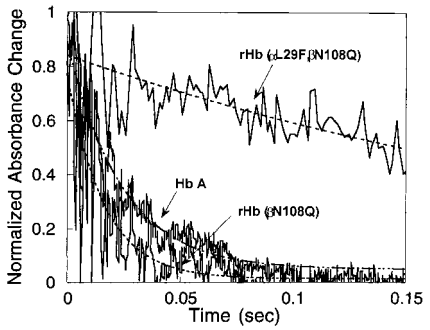

FIGURE 5: Normalized time courses for the reaction of oxy-Hb A and oxy-rHbs (0.4 μM after mixing) with 2 μM NO (after mixing) in 0.1 M phosphate buffer at pH 7.0 and 20 °C. The NO-induced oxidation rate constants were determined by NO concentration-dependent experiments. For clarity, the figure shows the normalized time courses for the reaction of only oxy-Hb A, oxy-rHb (βN108Q), and oxy-rHb (αL29F, βN108Q) with 2 μM NO. The time course of rHb (αL29F, βN108Q) overlaps that of rHb (αL29F).

The resonances at approximately −1.8 and −1.7 ppm have been assigned to the γ_2-CH_3 of the E11Val of the β-chain and the α-chain of HbCO A, respectively (*31, 41*). These two resonances are not changed in rHbCO (βN108Q); however, the resonance assigned to the γ_2-CH_3 of the α-E11Val of rHbCO (αL29F, βN108Q) is shifted upfield to approximately −2.0 ppm, suggesting that this group in rHbCO (αL29F, βN108Q) is located closer to the normal of the heme than in HbCO A. α29L is in close proximity to E11Val; hence, the amino acid substitution, αL29F, is

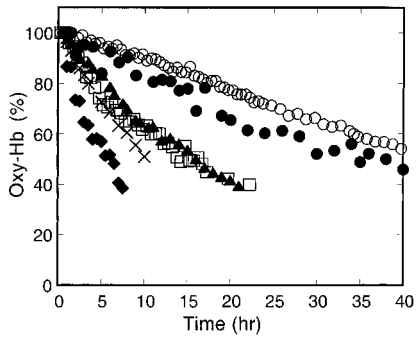

FIGURE 6: Autoxidation of (○) Hb A, (●) rHb (αL29F, βN108Q), (□) rHb (αL29F, αV96W, βN108K), (▲) rHb (βN108Q), (×) rHb (αV96W), and (◆) rHb (αV96W, βN108K) in PlasmaLyte buffer in the presence of 5 mM EDTA and 5% D_2O at pH 7.4 and 37 °C. The autoxidation process was measured by monitoring the rate of disappearance of the oxy-marker at −2.34 ppm upfield from DSS by 300-MHz ^{1}H NMR.

Table 3: Autoxidation Rate Constants, Oxygen Affinity, and Cooperativity of Low-Oxygen-Affinity Mutants

hemoglobin	k_{auto} (h^{-1})[a]	P_{50} (mmHg)[b]	n_{max}[b]
Hb A	0.0158 ± 0.0002	9.64	3.28
rHb (βN108Q)	0.0449 ± 0.0007	17.46	3.10
rHb (αL29F, βN108Q)	0.0181 ± 0.0006	12.06	2.77
rHb (αV96W)	0.0689 ± 0.0008	16.38	2.94
rHb (αV96W, βN108K)	0.125 ± 0.0051	50.65	2.36
rHb (αL29F, αV96W, βN108K)	0.0449 ± 0.0014	21.97[c]	1.81[c]

[a] Rate constants for the autoxidation (k_{auto}) of Hb A and rHbs were obtained at [oxy-Hb] = 3 mM (in terms of heme) in PlasmaLyte buffer at pH 7.4 and 37 °C. [b] Oxygen affinity and cooperativity were obtained in 0.1 M sodium phosphate buffer at 29 °C and pH 7.4. Protein concentrations were 0.1 mM heme. [c] Taken from Jeong et al. (*14*).

expected to alter the conformation of the distal heme pocket site of the α-chain. There are some other changes in the ring-current-shifted resonances among these rHbs. Our experience has been that minor differences in the intensity and positions of ring-current-shifted resonances are common features in many rHb mutants that we have studied (*1*−*5*, *37*−*39*, *42*). These changes reflect slight adjustments of the conformation of the hemes and/or the amino acid residues in the heme pockets as a result of the mutation.

The exchangeable proton resonances of the Hb molecule arise from the exchangeable protons in the subunit interfaces. Of special interest to this study are the exchangeable proton resonances at 14.2, 12.9, 12.1, 11.2, and 10.7 ppm from DSS,

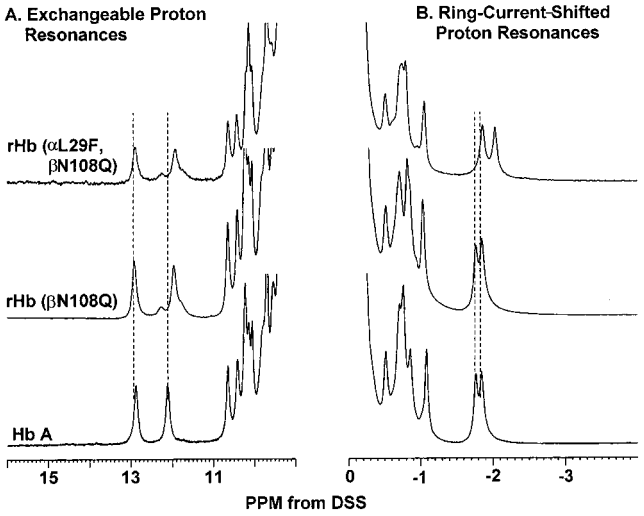

FIGURE 7: 500-MHz ^{1}H NMR spectra of rHbs and Hb A in the CO form in 0.1 M sodium phosphate buffer at pH 7.0 and 29 °C.

which have been characterized as the intersubunit H-bonds in the $\alpha_1\beta_1$ and $\alpha_1\beta_2$ subunit interfaces in both deoxy (T) and/or oxy (R) states of Hb A (*36*, *43*, *44*). The resonances at 12.9 and 12.1 ppm from DSS have been assigned to the H-bonds between α122His and β35Tyr and α103His and β131Gln, respectively (*44*, *45*; C.-K. Chang and C. Ho, unpublished results). In the spectra of rHbCO (βN108Q) and rHbCO (αL29F, βN108Q) (Figure 7), three resonances instead of one occur corresponding to the chemical shift of HbCO A at 12.1 ppm. The main peak occurs at 12.0 ppm, with a shoulder at 11.8 ppm and an extra resonance at 12.3 ppm. The intensities of the resonances at 12.3 and 11.8 ppm are not even 1/10th of the ones at 12.0 and 12.9 ppm, indicating that these two extra resonances are unlikely to be contributed by additional protons. The sum of the integrated areas of the resonances at 11.8, 12.0, and 12.3 ppm is about the same as the area of the single resonance at 12.9 ppm, suggesting the coexistence of three conformers of rHb (βN108Q) in the CO form.

Figure 8 shows the hyperfine-shifted resonances and exchangeable proton resonances of rHbs and Hb A in the deoxy form. The resonance at 63 ppm from DDS has been assigned to the hyperfine-shifted N_δH-exchangeable proton of the proximal histidine residue of the α-chain (α87His) of deoxy-Hb A, and the one at 77 ppm from DSS has been assigned to the corresponding residue of the β-chain (β92His) of deoxy-Hb A (Figure 8A) (*46*, *47*). The chemical shift positions of these two proximal histidyl resonances in rHb (βN108Q) are exactly the same as those of Hb A, indicating no perturbations around the proximal histidine residues of this rHb. However, the resonance at 63 ppm from DSS of rHb (αL29F) and rHb (αL29F, βN108Q) is shifted 4 ppm downfield to 67 ppm, reflecting a change in the environment of the proximal heme pocket of the α-chain as a result of the mutation at αL29F.

The spectral region from 10 to 25 ppm arises from the hyperfine-shifted resonances of the porphyrin ring and the amino acid residues situated in proximity to the heme pockets and the exchangeable proton resonances (Figure 8B). There are no noticeable differences in the resonances from 10 to 25 ppm between deoxy-Hb A and deoxy-rHb (βN108Q). However, there are spectral changes in rHb (αL29F) and

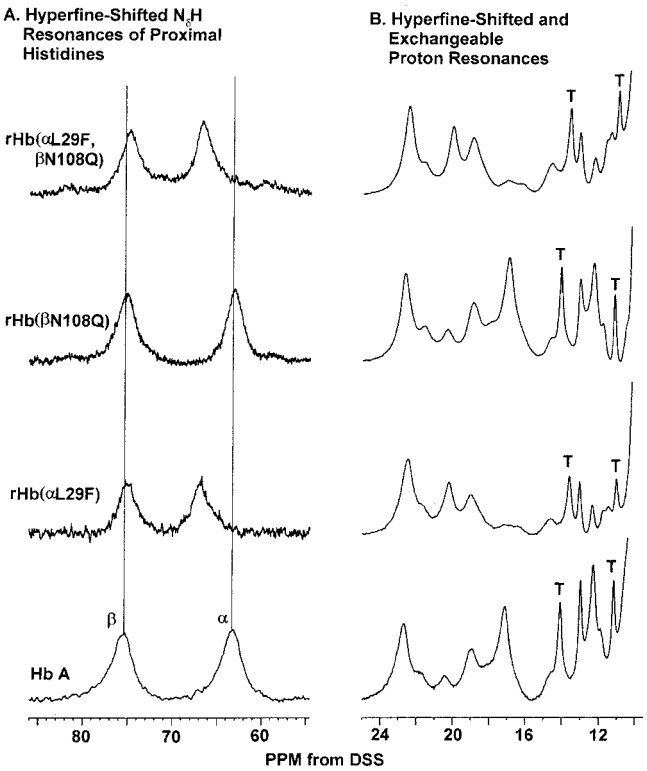

FIGURE 8: 300-MHz ^{1}H NMR spectra of rHbs and Hb A in the deoxy form in 0.1 M sodium phosphate buffer at pH 7.0 and 29 °C.

rHb (αL29F, βN108Q) over the region from 16 to 20 ppm, reflecting changes in the environment of the heme pockets of both the α- and the β-chains. The resonance at 14.2 ppm has been identified as the intersubunit H-bond between α42Tyr and β99Asp in the $\alpha_1\beta_2$ interface in deoxy Hb A (*43*), a characteristic feature of the deoxy (T) quaternary structure of Hb A (*48*). This resonance of rHb (αL29F) and rHb (αL29F, βN108Q) is shifted 0.5 ppm upfield to 13.7 ppm, indicating that this $\alpha_1\beta_2$ interface H-bond in the deoxy form is perturbed by the mutation at αL29F.

A unique feature of our rHbs with low oxygen affinity and high cooperativity is the appearance of the T-marker at ~14 ppm on lowering the temperature and/or adding IHP to these rHbs in the CO form (*3*−*5*). Studies on the temperature dependence of exchangeable proton resonances of rHbs in the CO form can be used to assess the structural effect on oxygen affinity. Figures 9 and 10 show the exchangeable proton resonances of rHb (βN108Q) and rHb (αL29F, βN108Q) in the CO form in the absence and presence of 4 mM IHP as a function of temperature. The resonance at 14.2 ppm of rHb (βN108Q) is observable starting at 23 °C (Figure 9B), and the resonance of rHb (αL29F, βN108Q) starts at 17 °C (Figure 10B) in the presence of 4 mM IHP. The appearance of the T-marker in the presence of 4 mM IHP at low temperature in the spectra of CO-ligated rHb (βN108Q) and rHb (αL29F, βN108Q) indicates that the T state of these rHbs is more stable than that of Hb A. This resonance in the spectra of Hb (αL29F, βN108Q) (Figure 10B) has a much smaller intensity than that in the spectra of rHb (βN108Q) (Figure 9B) at low temperature, i.e., 11 °C and in the presence of 4 mM IHP.

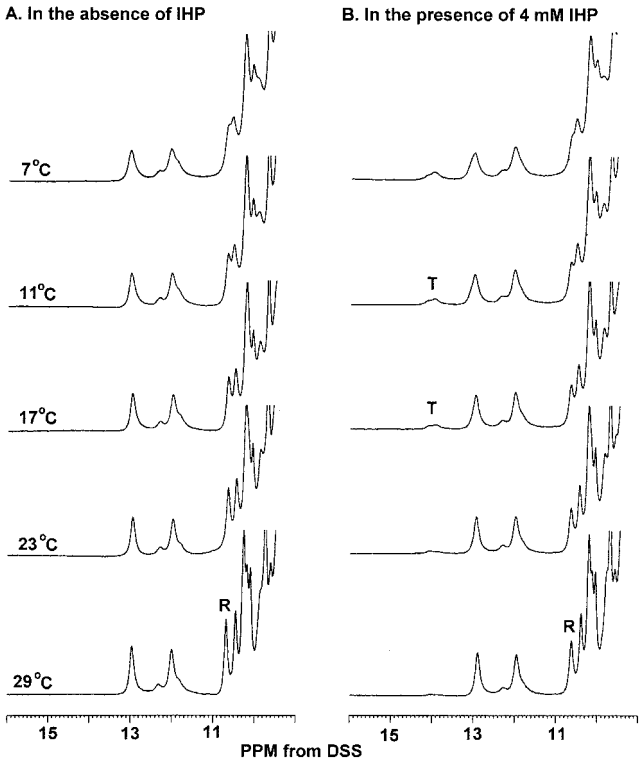

FIGURE 9: Effect of temperature and 4 mM IHP on the ^{1}H NMR spectra of the CO form of rHb (βN108Q) in 0.1 M sodium phosphate buffer at pH 7.0 measured at 500 MHz.

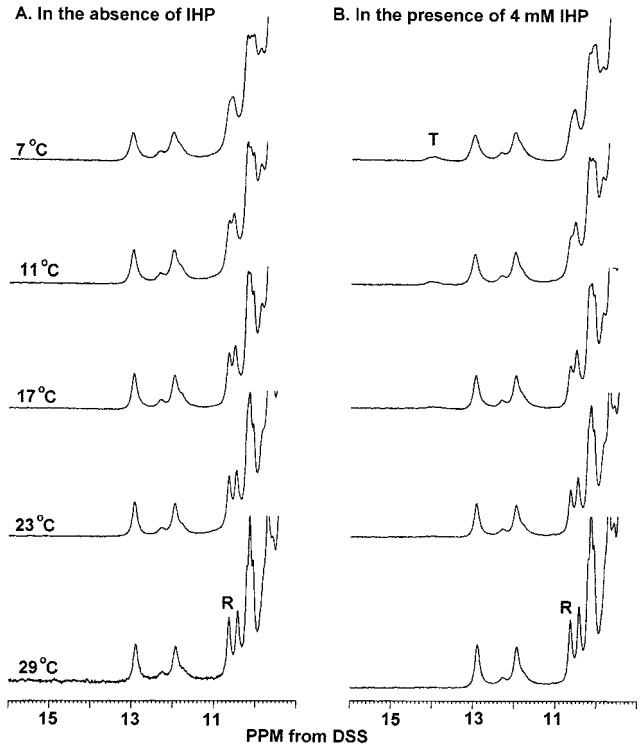

FIGURE 10: Effect of temperature and 4 mM IHP on the ^{1}H NMR spectra of the CO form of rHb (αL29F, βN108Q) in 0.1 M sodium phosphate buffer at pH 7.0 measured at 500 MHz.

DISCUSSION

In the present work, we have expressed and characterized two novel rHbs with amino acid substitutions in the $\alpha_1\beta_1$ interface (in the central cavity of the Hb molecule) and in the distal heme pocket of the α-chain, i.e., rHb (βN108Q) and rHb (αL29F, βN108Q). rHb (βN108Q) exhibits lower oxygen affinity and high cooperativity as compared to Hb A (Figures 1 and 2) and also exhibits slower autoxidation as compared to other known low-oxygen-affinity mutants (Table 3). ^{1}H NMR studies show that rHb (βN108Q) has similar tertiary structure around the heme pockets and quaternary structure in the $\alpha_1\beta_1$ and $\alpha_1\beta_2$ subunit interfaces as compared to those of Hb A (Figures 7 and 8). ^{1}H NMR studies also demonstrate that the R quaternary structure of rHb (βN108Q) can switch to the T quaternary structure with the ligands intact by lowering the ambient temperature and adding IHP. This indicates that the molecular basis for the low oxygen affinity of rHb (βN108Q) is that it favors the T conformation as compared to Hb A. Thus, rHb (βN108Q) follows a similar molecular mechanism for low oxygen affinity as other known low-oxygen-affinity mutants that we have studied in our laboratory (*3*−*5*, *14*).

In 0.1 M phosphate buffer at pH 7.4 and 29 °C, the mutation at βN108Q affects the initial stages of oxygenation the most [$\Delta\log P_{10} > \Delta\log P_{50}$; $\Delta\log P_{10,50} = \log P_{10,50}$ (mutant) − $\log P_{10,50}$ (Hb A)], resulting in asymmetric shifts away from the Hb A data (insert in Figure 3). The corresponding values of $\Delta\log P_{10}$ and $\Delta\log P_{50}$ were 0.296 and 0.259. This suggests that the first oxygen binds with much lower affinity to deoxy-rHb (βN108Q) than to deoxy-Hb A. This result is in agreement with our ^{1}H NMR studies, in which the T quaternary structure of rHb (βN108Q) is shown to be more stable than that of Hb A, resulting in lower oxygen affinity. In the presence of 5 mM 2,3-BPG, both the initial stages and the later stages of oxygenation are equally affected by the mutation rHb (βN108Q), resulting in symmetric shifts of the oxygen-binding curve of rHb (βN108Q) from that of Hb A under the same conditions. The corresponding values of $\Delta\log P_{10}$ and $\Delta\log P_{50}$ were 0.312 and 0.313 in the presence of 5 mM 2,3-BPG. The symmetric right shift in oxygen affinity of rHb (βN108Q) in the presence of 2,3-BPG results in preserved cooperativity with an n_{max} value of 3.2. Figure 3 also shows the effect of introduction of a bulky side chain Phe at αL29 on the oxygen-binding curve of rHb (βN108Q). Introduction of αL29F into βN108Q increases the oxygen-binding affinity in the initial oxygenation of rHb (βN108Q) more than in the later stage. Hence, as compared to Hb A, the initial stages of oxygenation are less affected by rHb (αL29F, βN108Q) ($\Delta\log P_{10} < \Delta\log P_{50}$; $\Delta\log P_{10} = 0.039$; $\Delta\log P_{50} = 0.095$). This is in agreement with the finding of Carver et al. (*9*), in which the oxygen affinity of Mb increases by 15-fold due to the mutation Leu→Phe at the B10 position.

X-ray studies of Brzozowski et al. (*49*) and Liddington et al. (*50*) show that oxygen is bound only to the α-hemes of single crystals in the deoxy quaternary structure. An optical spectroscopic study of oxygen binding to Hb A crystals further suggests that there is a 5-fold difference in oxygen-binding affinity between α- and β-hemes of single crystals in the deoxy structure (*51*). Quantification of the hyperfine-shifted exchangeable resonances assigned to the $N_\delta H$ of the proximal histidyl residues of Hb A in the deoxy form using ^{1}H NMR also shows that the α-chain of Hb A binds oxygen more strongly than the β-chain (*52*, *53*). These results are in agreement with the early observations of Ho and co-workers in which oxygen binds preferentially to the α-chain of Hb A in the presence of 2,3-BPG or IHP (*54*−*57*). As a first

approximation, one can assume at least at low oxygen saturation, O_2 binds to the α-chain first. Hence, the induced asymmetric shift of the oxygen-binding curve of rHb (βN108Q) (insert in Figure 3) is interpreted as a result of lowered oxygen affinity of the α-chain in rHb (βN108Q). The introduction of αL29F into rHb (βN108Q) increases the oxygen affinity of the α-chain and, hence, results in increasing the initial stage of oxygenation more than the later stage. β108 (G10) is located in the $\alpha_1\beta_1$ subunit interface, and substitution of Gln for Asn affects the oxygen affinity of the α-chain, especially in the initial stage of oxygenation. This suggests that there is communication between the $\alpha_1\beta_1$ and the $\alpha_1\beta_2$ subunit interfaces during the oxygenation process of the Hb molecule, as we have suggested previously (*5*).

The mutations rHb (βN108Q) and rHb (αL29F, βN108Q) have caused 1.2- and 5.7-fold decreases in the initial rate of CO binding, respectively (Figure 4 and Table 2). This suggests that the mutations increase the barrier to the diffusion of the ligand, especially in rHb (αL29F, βN108Q) (*58*). In deoxy-Hb A, a noncoordinated water molecule is present in the heme pocket of the α-chains, whereas in the β-chains His (E7) and Val (E11) are collapsed over the heme (*59*). Ligand binding requires the displacement of the bound water that is hydrogen bonded to the N_ϵ atom of distal histidine (E7) and the entry of ligand (*58*). Our ^{1}H NMR studies of deoxy-rHb (αL29F, βN108Q) show a change in the environment of the proximal heme pocket of the α-chain. (Figure 8). Also, the γ_2-CH_3 group of the α-E11 valine residues in rHbCO (αL29F, βN108Q) is suggested to be located closer to the normal of the heme than that in HbCO A as seen by its larger ring-current-shifted effect observed in ^{1}H NMR (Figure 7). These results suggest that the heme of rHb (αL29F, βN108Q) is likely to be sterically hindered, and this results in a lower CO-binding rate constant.

Carver et al. (*9*) reported that, in Mb, a 10-fold decrease in autoxidation rate is accompanied by a 15-fold increase in oxygen affinity in the B10 position mutation (Leu→Phe). Unlike Mb, oxy-Hb A shows a biphasic autoxidation reaction with fast and slow components, in which the α-chain is oxidized more rapidly than the β-chain (*60*). When we added the mutation αL29F to Hb A, rHb (αV96W, βN108K), and rHb (βN108Q), the autoxidation rates were decreased by 2-, 2.7-, and 2.5-fold, respectively (*14*; the present study). Thus, αL29F is shown to be effective in slowing down the autoxidation process of Hb A and rHbs as suggested by the results in Mb (*9*). It was noted that the formation of two sharp resonances at 23 and 37 ppm from DSS started during the first 30 min in the autoxidation process of rHb (αL29F, αV96W, βN108K) (results not shown). Also, resonances at 15 and 18 ppm started to build up together with these two resonances at 23 and 37 ppm after 3 h in the autoxidation process. The appearance of these proton resonances in the ^{1}H NMR spectra of met-rHb (αL29F, αV96W, βN108K) is suggestive of the formation of the anionic form of bishistidine hemichrome (*14*). However, hemichrome-like spectra are not observed in the autoxidation process of rHb (αL29F, βN108Q) (results not shown). Hence, the distal heme pocket structure of met-rHb (αL29F, βN108Q) is not favorable for the formation of hemichrome.

As seen in Table 2, rHb (βN108Q) increases the NO-induced oxidation rate by 1.2-fold as compared to Hb A. When we introduce the mutation αL29F into Hb A and rHb (βN108Q), there are 12- and 18.6-fold decreases in the NO-induced oxidation rate constant, respectively. Hence, αL29F is shown to be effective in slowing down the NO-induced oxidation process as suggested by Eich et al. (*11*). In a recent paper, Doherty et al. (*13*) demonstrated that the reduction of the NO reaction with deoxy- and oxy-Hb A by appropriate mutations in the distal heme pocket was associated with reduction of the hypertensive effect recorded in vivo. Hypertensive effects are often seen during the administration of extracellular Hb-based oxygen carriers and have been attributed to disruption of the NO signaling pathway (*61*−*64*). Hence, we propose rHb (αL29F, βN108K), which has moderately low oxygen affinity and high cooperativity and is resistant to auto- and NO-induced oxidation, as a potential candidate for Hb-based carriers or therapeutics.

The side chain of Asn at β108 interacts freely with the water molecules of the central cavity in both the deoxy and oxy forms (*18*, *19*). Amino acid substitution at β108Asn with either charged (Asp, Lys, and Glu, Arg; C.-H. Tsai, N. T. Ho, and C. Ho, unpublished results) or uncharged (Gln) polar residues results in rHbs with low oxygen affinity, suggesting that solvation effects can play a role in regulating the oxygen affinity of the Hb molecule (*65*). That is, as the β108Asn residue is replaced by Gln, Lys, Arg, Asp, or Glu, the electrostatic interaction between the β108 residue and the water molecules in the central cavity of the Hb becomes progressively stronger. This results in an increase in the stability of the T state. rHb (βN108A) (C.-H. Tsai, N. T. Ho, and C. Ho, unpublished results) and Hb (βN108I) (*23*), however, are both found to exhibit lower oxygen affinity than Hb A. These results suggest that other interactions, e.g., van der Wall interactions with other amino acid residues, may dominate the unfavorable solvation effects as introduced by the hydrophobic amino acid substitution. Brucker (*66*) has recently published the crystal structures of rHb Presbyterian (βN108K) and the cross-linked rHb Presbyterian. His results suggest that the extra H-bond formed between β108Lys and β35Tyr in the deoxy state can contribute to lower oxygen affinity of rHb Presbyterian by stabilizing its T state. If Ala is substituted for Asn at β108, this substitution is unlikely to introduce an H-bond between β108Ala and β35Tyr. However, rHb (βN108A) also has a lower oxygen affinity as compared to Hb A (C.-H. Tsai, N. T. Ho, and C. Ho, unpublished results). Hence, the molecular basis of low oxygen affinity found in rHbs mutated at the β108 site appears to result from removing the destabilizing native asparagine. More research is needed in order to understand the molecular basis of low oxygen affinity found in rHbs mutated at β108 site.

In conclusion, on the basis of the systematic investigation of the structure and function of a series of amino acid substitutions at the β108Asn site, rHb (βN108Q) is found to exhibit low oxygen affinity, high cooperativity, and slower autoxidation as compared to other known low-oxygen-affinity mutants developed in our laboratory. With the availability of our Hb expression system (*1*, *2*) and the information on the structure and function of Hb A and various Hb mutants, we can introduce extra mutation(s) into rHb (βN108Q) in order to develop rHbs that are suitable as Hb-based therapeutics and to gain further understanding of the oxygenation process of Hb.

ACKNOWLEDGMENT

We thank Dr. Ming F. Tam for carrying out N-terminal analyses by Edman degradation and electrospray ionization mass spectrometric analyses to evaluate the quality of the recombinant hemoglobins used in this study. We also thank Dr. E. Ann Pratt for helpful discussions.

REFERENCES

1. Shen, T.-J., Ho, N. T., Simplaceanu, V., Zou, M., Green, B. N., Tam, M. F., and Ho, C. (1993) *Proc. Natl. Acad. Sci. U.S.A. 90*, 8108−8112.
2. Shen, T.-J., Ho, N. T., Zou, M., Sun, D. P., Cottam, P. F., Simplaceanu, V., Tam, M. F., Bell, D. A., Jr., and Ho, C. (1997) *Protein Eng. 10*, 1085−1097.
3. Kim, H.-W., Shen, T.-J., Sun, D. P., Ho, N. T., Madrid, M., and Ho, C. (1995) *J. Mol. Biol. 248*, 867−882.
4. Ho, C., Sun, D. P., Shen, T.-J., Ho, N. T., Zou, M., Hu, C.-K., Sun, Z.-Y., and Lukin, J. A. (1998) in *Present and Future Perspectives of Blood Substitutes* (Tsuchida, E., Ed.) pp 281−296, Elsevier Science SA, Lausanne, Switzerland.
5. Tsai, C.-H., Shen, T.-J., Ho, N. T., and Ho, C. (1999) *Biochemistry 38*, 8751−8761.
6. Dickerson, R. E., and Geis, I. (1983) *Hemoglobin: Structure, Function, Evolution, and Pathology*, Benjamin/Cummings, Menlo Park, CA.
7. Di Iorio, E. E., Winterhalter, K. H., Mansouri, A., Blumberg, W. E., and Peisach, J. (1984) *Eur. J. Biochem. 145*, 549−554.
8. Ji, X., Karavitis, M., Razynska, A., Kwansa, H., Vásquez, G., Fronticelli, C., Bucci, E., and Gilliland, G. L. (1998) *Biophys. Chem. 70*, 21−34.
9. Carver, T. E., Brantley, R. E., Jr., Singleton, E. W., Arduini, R. M., Quillin, M. L., Phillips, G. N., Jr., and Olson, J. S. (1992) *J. Biol. Chem. 267*, 14443−14450.
10. Brantley, R. E., Jr., Smerdon, S. J., Wilkinson, A. J., Singleton, E. W., and Olson, J. S. (1993) *J. Biol. Chem. 268*, 6995−7010.
11. Eich, R. F., Li, T., Lemon, D. D., Doherty, D. H., Curry, S. R., Aitken, J. F., Mathews, A. J., Johnson, K. A., Smith, R. D., Phillips, G. N., Jr., and Olson, J. S. (1996) *Biochemistry 35*, 6976−6983.
12. Olson, J. S., Eich, R. F., Smith, L. P., Warren, J. J., and Knowles, B. C. (1997) *Artif. Cells, Blood Substitutes, Immobilization Biotechnol. 25*, 227−241.
13. Doherty, D. H., Doyle, M. P., Curry, S. R., Vali, R. J., Fattor, T. J., Olson, J. S., and Lemon, D. D. (1998) *Nat. Biotechnol. 16*, 672−676.
14. Jeong, S. T., Ho, N. T., Hendrich, M. P., and Ho, C. (1999) *Biochemistry 38*, 13433−13442.
15. Levy, A., Kuppusamy, P. K., and Rifkind, J. M. (1990) *Biochemistry 29*, 9311−9316.
16. Levy, A., Sharma, V. S., Zhang, L., and Rifkind, J. M. (1992) *Biophys. J. 61*, 750−755.
17. Blumberg, W. E., and Peisach, J. (1991) *Adv. Chem. Ser. 100*, 271−291.
18. Tame, J. R. H., and Vallone, B. (2000) *Acta Crystallogr. D*56, 805−811.
19. Shaanan, B. (1983) *J. Mol. Biol. 171*, 31−59.
20. Moo-Penn, W. F., Wolff, J. A., Simon, G., Vacek. M., Jue, D. L., and Johnson, M. H. (1978) *FEBS Lett. 92*, 53−56.
21. Imamura, T., Fujita, S., Ohta, M., Hanada, M., and Yanase, T. (1969) *J. Clin. Invest. 48*, 2341−2348.
22. Huisman, T. H. J., Carver, M. F. H., and Efremov, G. D. (1998), in *A Syllabus of Human Hemoglobin Variants*, 2nd ed., p 241, The Sickle Cell Anemia Foundation, Augusta, GA.
23. Frischknecht, H., Speich, R., Bloch, K. E., Fehr, J., Tuchschmid, P., and Jenni, R. (1999) *Hemoglobin 23*, 83−87.
24. O'Donnell, J. K., Brich, P., Parsons, C. T., White, S. P., Okabe, J., Martin, M. J., Adams, C., Sundarapandiyan, K., Manjula, B. N., Acharya, A. S., Logan, J. S., and Kumar, R. (1994) *J. Biol. Chem. 269*, 27692−27699.
25. Hayashi, A., Suzuki, T., and Shih, M. (1973) *Biochim. Biophys. Acta 310*, 309−316.
26. Antonini, E. (1965) *Physiol. Rev. 45*, 123−170.
27. Mathews, A. J., Rohlfs, R. J., Olson, J. S., Tame, J., Renaud, J.-P., and Nagai, K. (1989) *J. Biol. Chem. 264*, 16573−16583.
28. Mathews, A. J., and Olson, J. S. (1994) *Methods. Enzymol. 232*, 363−386.
29. Plateau, P., and Guéron, M. (1982) *J. Am. Chem. Soc. 104*, 7310−7311.
30. Lindstrom, T. R., and Ho, C. (1973) *Biochemistry 12*, 134−139.
31. Dalvit, C., and Ho, C. (1985) *Biochemistry 24*, 3398−3407.
32. Wyman, J. (1948) *Adv. Protein Chem. 4*, 407−531.
33. Wyman, J. (1964) *Adv. Protein Chem. 19*, 223−286.
34. Mathews, A. J., Olson, J. S., Renaud, J.-P., Tame, J., and Nagai, K. (1991) *J. Biol. Chem. 266*, 21631−21639.
35. Rohlfs, R. J., Bruner, E., Chiu, A., Gonzales, A., Gonzales, M. L., Magde, D., Magde, M. D., Jr., Vandegriff, K. D., and Winslow, R. M. (1998) *J. Biol. Chem. 273*, 12128−12134.
36. Ho, C. (1992) *Adv. Protein Chem. 42*, 153−312.
37. Kim, H.-W., Shen, T.-J., Sun, D. P., Ho, N. T., Madrid, M., Tam, M. F., Zou, M., Cottam, P. F., and Ho, C. (1994) *Proc. Natl. Acad. Sci. U.S.A. 91*, 11547−11551.
38. Kim, H.-W., Shen, T.-J., Ho, N. T., Zou, M., Tam, M. F., and Ho, C. (1996) *Biochemistry 35*, 6620−6627.
39. Ho, C., Willis, B. F., Shen, T.-J., Ho, N. T., Sun, D. P., Tam, M. F., Suzuka, S. M., Fabry, M. E., and Nagel, R. L. (1996) *J. Mol. Biol. 263*, 475−485.
40. Barrick, D., Ho, N. T., Simplaceanu, V., Dahlquist, F. W., and Ho, C. (1997) *Nat. Struct. Biol. 4*, 78−83.
41. Lindstrom, T. R., Norén, I. B. E., Charache, S., Lehmann, H., and Ho, C. (1972) *Biochemistry 11*, 1677−1681.
42. Sun, D. P., Zou, M., Ho, N. T., and Ho, C. (1997) *Biochemistry 36*, 6663−6673.
43. Fung, L. W.-M., and Ho, C. (1975) *Biochemistry 14*, 2526−2535.
44. Russu, I. M., Ho, N. T., and Ho, C. (1987) *Biochim. Biophys. Acta 914*, 40−48.
45. Simplaceanu, V., Lukin, J. A., Fang, T.-Y., Zou, M., Ho, N. T., and Ho, C. (2000) *Biophys. J. 79*, 1146−1154.
46. Takahashi, S., Lin, A. K.-L. C., and Ho, C. (1980) *Biochemistry 19*, 5196−5202.
47. La Mar, G. N., Nagai, K., Jue, T., Budd, D., Gersonde, K., Sick, H., Kagimoto, T., Hayashi, A., and Taketa, F. (1980) *Biochem. Biophys. Res. Commun. 96*, 1172−1177.
48. Perutz, M. F. (1970) *Nature (London) 228*, 726−739.
49. Brzozowski, A., Derewenda, Z., Dodson, E., Dodson, G., Grabowski, M., Liddington, R., Skarzynski, T., and Vallely, D. (1984) *Nature* (*London*) *307*, 74−76.
50. Liddington, T. R., Derewenda, Z., Dodson, G., and Harris, D. (1988) *Nature* (*London*) *331*, 725−728.
51. Rivetti, C., Mozzarelli, A., Rossi, G. L., Henry, E. R., and Eaton, W. A. (1993) *Biochemistry 32*, 2888−2906.
52. Yao, C., Simplaceanu, V., Lin, A. K.-L. C., and Ho, C. (1986) *J. Magn. Reson. 66*, 43−57.
53. Fetler, K. B., Simplaceanu, V., and Ho, C. (1995) *Biophys. J. 68*, 681−693.
54. Johnson, M. E., and Ho, C. (1974) *Biochemistry 13*, 3653−3661.
55. Viggiano, G., and Ho, C. (1979) *Proc. Natl. Acad. Sci. U.S.A. 76*, 3673−3677.
56. Viggiano, G., Ho, N. T., and Ho, C. (1979) *Biochemistry 18*, 5238−5247.
57. Ho, C., Lam, C.-H. J., Takahashi, S., and Viggiano, G. (1982) in *Hemoglobin and Oxygen Binding* (Ho, C., Eaton, W. A., Collmann, J. P., Gibson, Q. H., Leigh, L. S., Jr., Margoliash, E., Moffat, K., and Schedit, W. R., Eds.), pp 141−149, Elsevier/North-Holland, New York, .
58. Olson, J. S., and Phillips, G. N. (1996) *J. Biol. Chem. 271*, 17593−17596.
59. Kavanaugh, J. S., Rogers, P. H., and Arnone, A. (1992) *Biochemistry 31*, 8640−8649.

60. Mansouri, A., and Winterhalter, K. H. (1973) *Biochemistry 12*, 4946−4949.
61. Hess, J. R., MacDonald, V. W., and Brinkley, W. W. (1993) *J. Appl. Physiol. 74*, 1769−1778.
62. Lee, R., Neya, K., Svizzero., T. A., and Vlahakes, G. J. (1995) *J. Appl. Physiol. 79*, 236−242.
63. Lieberthal, W., Wolf, E. F., Merrill, E. W., Levinsky, N. G., and Valeri, C. R. (1987) *Life Sci. 41*, 2525−2533.
64. Vandegriff, K. D., and Winslow, R. M. (1995) in *Blood Substitutes*, Birkhauser, Boston.
65. Colombo, M. F., Rau, D. C., and Parsegian, V. A. (1992) *Science 256*, 655−659.
66. Brucker, E. A. (2000) *Acta Crystallogr. D56*, 812−816.

BI001116A